

# Broad-band continuum and line emission of the $\gamma$ -ray blazar PKS 0537–441

E. Pian<sup>1</sup>, R. Falomo<sup>2</sup>, R. C. Hartman<sup>3</sup>, L. Maraschi<sup>4</sup>, F. Tavecchio<sup>4</sup>, M. Tornikoski<sup>5</sup>, A. Treves<sup>6</sup>, C. M. Urry<sup>7</sup>,  
L. Ballo<sup>4</sup>, R. Mukherjee<sup>8</sup>, R. Scarpa<sup>9</sup>, D. J. Thompson<sup>3</sup>, and J. E. Pesce<sup>10</sup>

<sup>1</sup> Osservatorio Astronomico di Trieste, Via G.B. Tiepolo 11, 34131 Trieste, Italy

<sup>2</sup> Osservatorio Astronomico di Padova, via dell'Osservatorio 5, 35122 Padova, Italy

<sup>3</sup> NASA Goddard Space Flight Center, Greenbelt, MD 20771, USA

<sup>4</sup> Osservatorio Astronomico di Brera, via Brera 28, 20121 Milano, Italy

<sup>5</sup> Metsahovi Radio Observatory, Metsahovintie 114, 02540 Kylmala, Finland

<sup>6</sup> Dipartimento di Scienze, University of Insubria, Via Valleggio 11, 22100 Como, Italy

<sup>7</sup> Department of Physics, Yale University, PO Box 208121, New Haven, CT 06520-8121, USA

<sup>8</sup> Department of Physics and Astronomy, Barnard College, Columbia University, New York, NY 10027, USA

<sup>9</sup> European Southern Observatory, 3107 Alonso de Cordova, Santiago, Chile

<sup>10</sup> Eureka Scientific and George Mason University, 4400 University Drive, Fairfax, Virginia, VA 22030, USA

Received 19 February 2002 / Accepted 10 June 2002

**Abstract.** PKS 0537–441, a bright  $\gamma$ -ray emitting blazar, was observed at radio, optical, UV and X-ray frequencies during various EGRET pointings, often quasi-simultaneously. In 1995 the object was found in an intense emission state at all wavelengths. BeppoSAX observations made in 1998, non-simultaneously with exposures at other frequencies, allow us to characterize precisely the spectral shape of the high energy blazar component, which we attribute to inverse Compton scattering. The optical-to- $\gamma$ -ray spectral energy distributions at the different epochs show that the  $\gamma$ -ray luminosity dominates the bolometric output. This, together with the presence of optical and UV line emission, suggests that, besides the synchrotron self-Compton mechanism, the Compton upscattering of photons external to the jet (e.g., in the broad line region) may have a significant role in the production of high energy radiation. The multiwavelength variability can be reproduced by changes of the plasma bulk Lorentz factor. The spectrum secured by IUE in 1995 appears to be partially absorbed shortward of  $\sim 1700$  Å. However, this signature is not detected in the HST spectrum taken during a lower state of the source. The presence of intervening absorbers is not supported by optical imaging and spectroscopy of the field.

**Key words.** galaxies: active – BL Lacertae objects: individual: PKS 0537–441 – ultraviolet: galaxies – X-ray: galaxies – gamma rays: observations

## 1. Introduction

Radiation in the MeV-GeV energy range has been firmly detected by EGRET in 65 active galactic nuclei, all of blazar type (von Montigny et al. 1995; Hartman 1999; Hartman et al. 1999). The  $\gamma$ -ray emission, coupled to the small emitting volumes inferred by variability time scales, implies beaming in a relativistic jet (which makes the emitting regions transparent to  $\gamma$ -ray photons, e.g., McBreen 1979; Maraschi et al. 1992), a distinctive characteristic of blazars. Among EGRET blazars, many exhibit variability on a range of timescales from years to days (Wehrle et al. 1998; Mattox et al. 1997; Bloom et al. 1997; Hartman 1996; Hartman 1999).

There is a general consensus that the emission of blazars at energies higher than 10 MeV should be attributed to inverse Compton scattering of relativistic electrons off soft photons

produced in or in the vicinity of the jet. However, the exact role played in the scattering process by photons created in the jet (synchrotron photons) or outside (broad emission line region or accretion disk photons) is not known, nor is the cause of the huge, dramatic  $\gamma$ -ray flares observed. Depending on which physical parameters are varying (electron density, magnetic field density, bulk Lorentz factor), variations of different amplitude are expected in the synchrotron and inverse Compton components (see Hartman et al. 1996; Wehrle et al. 1998; Ghisellini & Madau 1996; Ghisellini & Maraschi 1996). The most effective way to discriminate among the different scenarios consists in observing these sources simultaneously at several wavelengths spanning a broad range.

PKS 0537–441 ( $z = 0.896$ ) is one of the most luminous and variable blazars at all frequencies, and has been the target of monitoring from radio to X-rays at many epochs (Cruz-Gonzalez & Huchra 1984; Maraschi et al. 1985; Tanzi et al. 1986; O'Brien et al. 1988; Bersanelli et al. 1992;

Send offprint requests to: E. Pian,  
e-mail: pian@ts.astro.it

Edelson et al. 1992; Falomo et al. 1993a; Treves et al. 1993; Falomo et al. 1994; Romero et al. 1994; Heidt & Wagner 1996; Tingay et al. 1996; Sefako et al. 2000; Tornikoski et al. 2001; Romero et al. 2002). The source was detected by EGRET for the first time in 1991 (Michelson et al. 1992; Thompson et al. 1993), and then re-observed at many successive epochs. It is bright and variable in  $\gamma$ -rays, and its luminosity in the highest state is comparable to the average luminosity of the strongest and best studied EGRET blazar, 3C 279. Multiwavelength modeling, based on non-simultaneous  $\gamma$ -ray and lower frequencies data, has been proposed by Maraschi et al. (1994a) within the synchrotron self-Compton scheme.

On the basis of its radio variability characteristics (Romero et al. 1995) and an off-centered surrounding nebulosity (Stickel et al. 1988), it was proposed that PKS 0537–441 is microlensed by stars in a foreground galaxy (see however Romero et al. 2000). Search for extended optical emission around PKS 0537–441 has a long and controversial history (e.g., Falomo et al. 1992; Lewis & Ibatá 2000; Scarpa et al. 2000). Clarifying the nature of this emission is of importance both for the study of the properties of the galaxy and environment hosting this very active nucleus and for the alleged possibility of microlensing effects.

In this paper we present multiwavelength observations of PKS 0537–441 at various epochs during the EGRET lifetime, and particularly focus on the  $\gamma$ -ray flare of 1995 (Sect. 2.1). We also report on 1998 BeppoSAX observations in the 0.2–50 keV band (Sect. 2.2) and consider archival HST spectra (Sect. 2.3). In Sect. 2.4.2 we compare and discuss the results of all imaging studies of the field. In Sect. 3 we discuss the overall energy distribution and its implications for the nuclear emission mechanisms.

## 2. Observations, data analysis and results in individual bands

### 2.1. $\gamma$ -rays

PKS 0537–441 was repeatedly observed in the band 0.03–10 GeV by EGRET aboard CGRO: a summary of the observations, with flux levels or upper limits, is reported in the 3rd EGRET catalog (Hartman et al. 1999). We have re-analyzed the July–August 1991 spectrum with up-to-date software and obtain a marginally steeper slope (see Table 1) than found by Thompson et al. (1993). During January 1995 the source was detected with almost  $10\text{-}\sigma$  significance, with an average flux of  $90 \times 10^{-8}$  photons  $\text{s}^{-1} \text{cm}^{-2}$ , its brightest recorded  $\gamma$ -ray state (see Hartman et al. 1999 for details of the data reduction and analysis). The high signal-to-noise ratio of the detection allowed a rather detailed spectral analysis (see Mukherjee et al. 1997 and Table 1) and a study of the variability on a day time scale. In Fig. 1 we report the EGRET light curve of the blazar during the January 1995 pointing, with a temporal binning of 2 days (see also Hartman 1996). Toward the end of the monitoring, the flux increases in  $\sim 2$  days by a factor of at least  $\sim 3$  with respect to the average level during the first 10 days of the observation. The target was detected by EGRET also three months

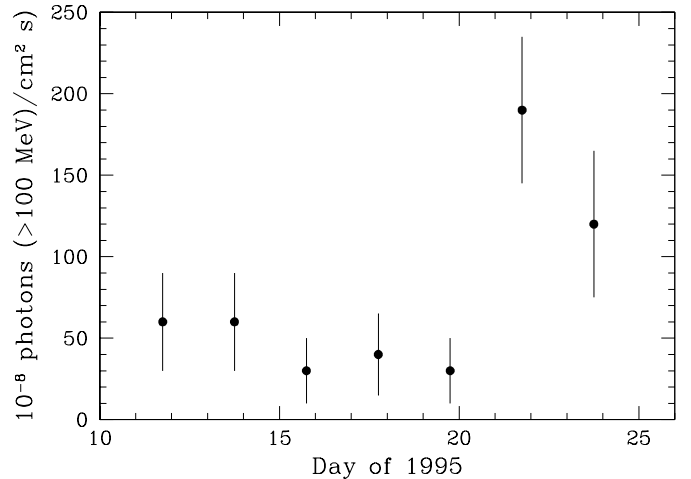


Fig. 1. EGRET light curve of PKS 0537–441 in January 1995.

later, in a state  $\sim 4$  times lower than shown here (Hartman et al. 1999).

In Table 1 and Fig. 2 we report the EGRET data taken quasi-simultaneously (within  $\sim 6$  months) with data at lower frequencies. The January 1995 spectrum is significantly flatter than measured in 1991, consistent with a common characteristics of  $\gamma$ -ray blazars, which tend to have flatter spectra during flare states (Sreekumar et al. 1996; Sreekumar et al. 2001).

### 2.2. X-rays

X-ray observations of PKS 0537–441 prior to 1991 are summarized by Treves et al. (1993). The results of the ROSAT 1991 observation presented by those authors are reported in Table 1 and Fig. 2.

We observed PKS 0537–441 with BeppoSAX in 1998 November 28.3142–30.5291 (UT) as part of a program focussed on BL Lacs with flat X-ray spectra, supposedly dominated by the inverse Compton component. The total on-source integration times were 23 672, 47 396, and 36 743 s for the LECS (0.1–4 keV), MECS (1.6–10 keV) and PDS (13–300 keV) instruments, respectively (see Scarsi 1993 and Boella et al. 1997 for overviews of the BeppoSAX satellite).

The spectra taken by the LECS and MECS instruments have been extracted from the linearized event files using radii of  $8''$  and  $4''$ , respectively, and corrected for background contamination with library files available at the BeppoSAX Science Data Center. The net count rates, averaged over the whole pointing, are  $(1.93 \pm 0.11) \times 10^{-2}$  cts  $\text{s}^{-1}$  in the LECS and  $(2.37 \pm 0.08) \times 10^{-2}$  cts  $\text{s}^{-1}$  in the MECS. The spectra measured by the PDS instrument have been accumulated from on source exposures of the collimator units, and corrected using background spectra obtained during the off-source exposures. A correction for the energy and temperature dependence of the pulse rise time has been also applied (Frontera et al. 1997). The average PDS spectrum of the source exhibits significant signal up to  $\sim 30$  keV and appears featureless; its net count rate is

**Table 1.** Multiwavelength observations of PKS 0537–441.

Date	Instrument	$\alpha_v^a$	$F_v^b$	$\nu^c$	Ref. <sup>d</sup>
1991 Feb. 11	ESO 1.5 m+CCD	$1.35 \pm 0.05$	$2.19 \pm 0.04$ mJy	$5.45 \times 10^{14}$	1
1991 Apr. 16	ROSAT+PSPC	$1.1 \pm 0.4$	$0.79 \pm 0.05$ $\mu$ Jy	$2.41 \times 10^{17}$	2
1991 Jul. 26-Aug. 08	CGRO+EGRET	$1.50 \pm 0.32$	$39 \pm 8$ pJy	$9.66 \times 10^{22}$	3, 4
1992 May 14-Jun. 04	CGRO+EGRET	...	$<48^e$ pJy	$9.66 \times 10^{22}$	5
1992 May 21.41	IUE+LWP	...	$0.66 \pm 0.05^f$ mJy	$1.15 \times 10^{15}$	4
1992 May 21.55	IUE+LWP	...	$0.78 \pm 0.03^f$ mJy	$1.15 \times 10^{15}$	4
1993 Jul. 12	HST+FOS+G130H	...	$0.09 \pm 0.01^f$ mJy	$2.14 \times 10^{15}$	4
1993 Sep. 16	HST+FOS+G270H	$1.92 \pm 0.09$	$0.371 \pm 0.007^f$ mJy	$1.15 \times 10^{15}$	4
1995 Jan. 10-24	CGRO+EGRET	$0.96 \pm 0.18$	$137 \pm 21$ pJy	$9.66 \times 10^{22}$	6
1995 Jan. 30.37	IUE+SWP	$1.2 \pm 0.1^g$	$0.90 \pm 0.02^f$ mJy	$1.67 \times 10^{15}$	4
1995 Jan. 31.44	IUE+LWP	$1.2 \pm 0.1^g$	$1.45 \pm 0.08^f$ mJy	$1.15 \times 10^{15}$	4
1995 Feb. 01.17	ESO SEST	...	$5.16 \pm 0.21$ Jy	$90 \times 10^9$	4
1995 Feb. 03	ESO 1.5 m+CCD	$1.29 \pm 0.04$	$3.03 \pm 0.15$ mJy	$5.45 \times 10^{14}$	7
1995 Feb. 05	ESO 1.5 m+CCD	$1.27 \pm 0.05$	$3.64 \pm 0.20$ mJy	$5.45 \times 10^{14}$	7
1995 Feb. 07	ESO 1.5 m+CCD	$1.09 \pm 0.04$	$5.26 \pm 0.25$ mJy	$5.45 \times 10^{14}$	7
1995 Feb. 27.14	ESO SEST	...	$2.88 \pm 0.23$ Jy	$230 \times 10^9$	4
1998 Nov. 28–30	BeppoSAX	$0.80 \pm 0.13$	$0.46 \pm 0.09$ $\mu$ Jy	$2.41 \times 10^{17}$	4

<sup>a</sup> Spectral index ( $F_\nu \propto \nu^{-\alpha_\nu}$ ). Uncertainties, both for  $\alpha$  and fluxes, are at 90% confidence level for the X- and  $\gamma$ -ray measurements, and at 68% for UV, optical and millimetric. No spectral fit has been tried when the data signal-to-noise ratio was too low or the spectral range too limited.

<sup>b</sup> Flux density. EGRET flux conversion follows Thompson et al. (1996). Optical-to-X-ray data are corrected for Galactic extinction.

<sup>c</sup> Frequency to which the flux density refers, in Hz.

<sup>d</sup> References. **1:** Falomo et al. (1994); **2:** Treves et al. (1993); **3:** Thompson et al. (1993); **4:** This paper; **5:** Hartman et al. (1999); **6:** Mukherjee et al. (1997); **7:** Scarpa & Falomo (1997).

<sup>e</sup>  $2\text{-}\sigma$  upper limit.

<sup>f</sup> The uncertainty is only statistical. For IUE data, this was evaluated following Falomo et al. (1993b).

<sup>g</sup> From a spectral fit over the band 1700–5500 Å.

$(3.9 \pm 1.6) \times 10^{-2}$  cts  $s^{-1}$ . No emission variability larger than 15% has been detected within the pointing.

After rebinning the LECS, MECS and PDS spectra in intervals where the signal exceeds a  $3\text{-}\sigma$  significance, we fitted them to a single absorbed power-law using the XSPEC routines and response files available at the Science Data Center. The LECS and PDS spectra normalizations relative to the MECS have been treated as a free (best fit value  $0.86 \pm 0.09$ , within the expected range) and fixed (0.85) parameters, respectively, and the neutral hydrogen column density has been fixed to its Galactic value ( $N_{\text{HI}} = 2.91 \times 10^{20}$   $\text{cm}^{-2}$ , Murphy et al. 1996). The fit is satisfactory ( $\chi_\nu^2 = 0.6$ ). The best-fit power-law parameters are reported in Table 1 and the deconvolved de-absorbed X-ray fluxes in the BeppoSAX energy band are reported in Fig. 2. We also searched for a possible iron emission line corresponding to the  $K\alpha$  transition at the expected redshifted energy on the MECS spectrum, but we do not detect any line with intensity larger than  $1.4 \times 10^{-14}$   $\text{erg s}^{-1} \text{cm}^{-2}$  ( $3\sigma$  upper limit).

The spectrum and emission state detected by BeppoSAX are consistent with those measured at earlier epochs by EXOSAT and Einstein (Treves et al. 1993), while the BeppoSAX flux at 1 keV is almost a factor of  $\sim 2$  lower than that detected by ROSAT in 1991.

### 2.3. Ultraviolet

IUE performed low dispersion spectroscopy of PKS 0537–441 in the 2000–3000 Å (LWR or LWP cameras) and 1200–1950 Å (SWP) wavelength ranges at various epochs between 1980 and 1995, and in two occasions, May 1992 and January 1995, quasi-simultaneously with EGRET pointings (Table 1). The corresponding IUE spectra were retrieved from the INES<sup>1</sup> and NEWSIPS<sup>2</sup> (Nichols & Linsky 1996; Garhart et al. 1997) archives and, for the 1995 data only, extracted from the bidimensional spectral images with the GEX routine (Urry & Reichert 1988).

The INES and NEWSIPS spectra of May 1992 agree in flux to within  $\sim 10\%$ , and therefore can be considered consistent, given the low level of the source and the possible differences in background estimate between the two extraction methods. In Table 1 and Fig. 2 we have reported the results obtained with the NEWSIPS extraction. As a consistency check, we note that these UV fluxes are compatible with the power-law fitting the optical data taken more than one year earlier (see Table 1 and Fig. 2).

For the spectra of January 1995, the INES and NEWSIPS methods return compatible results for the IUE SWP range (the flux at 1800 Å, averaged between the two extractions and

<sup>1</sup> <http://ines.vilspa.esa.es/ines/docs/contents.html>

<sup>2</sup> <http://archive.stsci.edu/iue/index.html>

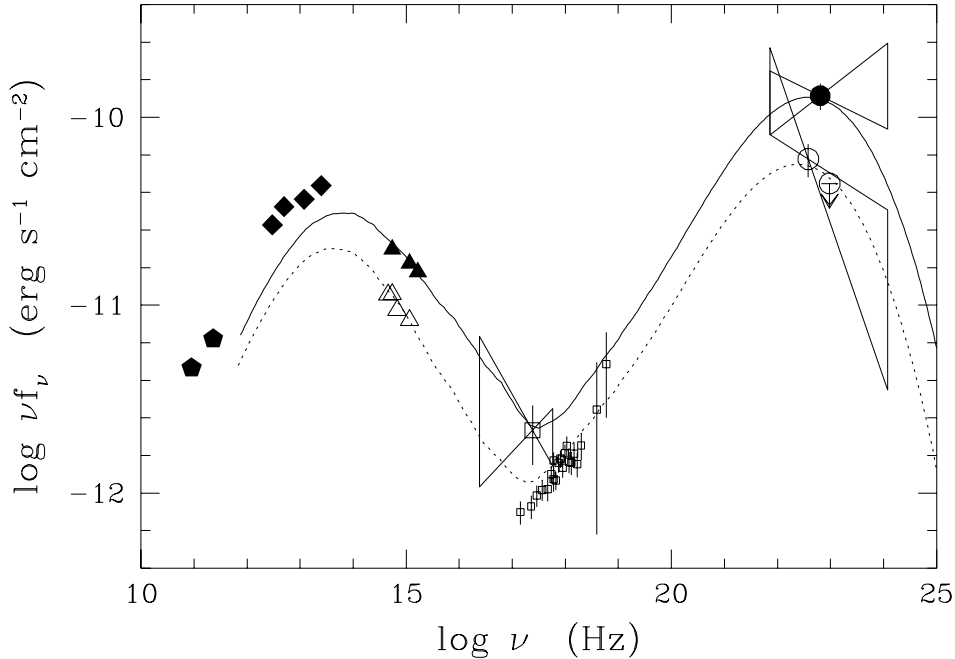


**Fig. 2.** Radio-to- $\gamma$ -ray spectral energy distribution of PKS 0537–441 at different states (see Table 1 for data references). The filled pentagons, triangles and circle represent millimetric, optical-to-UV and  $\gamma$ -ray data in Jan.-Feb. 1995, respectively; diamonds are IRAS 1984 data from Impey & Neugebauer (1988). The open triangles stand for optical February 1991 and UV 1992 data, open squares represent ROSAT April 1991 (large symbol) and BeppoSAX 1998 (small symbol) data, and open circles represent the EGRET Jul.-Aug. 1991 detection and 1992 upper limit. Data at optical-to-X-ray frequencies are corrected for Galactic extinction (see text). Superimposed on the multiwavelength data are the model curves for the low 1991-1992 state (dotted), and for the high 1995 state (solid). The model parameters for the low state are  $\gamma_{\min} = 1$ ,  $\gamma_b = 400$ ,  $\gamma_{\max} = 2.5 \times 10^4$ ,  $n_1 = 1.6$ ,  $n_2 = 4$ ,  $B = 3.5$  Gauss,  $K = 6 \times 10^3 \text{ cm}^{-3}$ ,  $R = 2.7 \times 10^{16} \text{ cm}$ ,  $\delta \simeq \Gamma = 10$  (see Ballo et al. 2002 for the parameter notation). In high state, the above parameters remain unchanged, except that  $\Gamma = 11$  and  $n_2 = 3.8$ . The external Compton seed photon source (disk photons reprocessed in the broad line region) is assumed to have a density  $U_{\text{ext}} = 6 \times 10^{-3} \text{ erg cm}^{-3}$ ; the disk temperature is assumed to be  $10^4 \text{ K}$ .

corrected for Galactic extinction, is  $1.21 \pm 0.03 \text{ mJy}$ ), while in the LWP range the NEWSIPS extracted flux is up to a factor of 2 higher than found with INES. The GEX extracted flux is  $\sim 25\%$  lower than that given by INES and NEWSIPS in the SWP band, and is consistent with the INES result in the LWP band. Since we have verified that the differences between pairs of IUE spectra of bright sources (e.g., the BL Lac object PKS 2155–304) extracted with different methods do not exceed 1–2% (see also Urry et al. 1993), we ascribe the discrepancies we find for PKS 0537–441 to the difficulty of correctly evaluating the background at UV flux levels comparable with the IUE sensitivity limit and of properly removing the solar scattered light, which critically contaminates the IUE LWP camera acquisitions after 1992 (Caplinger 1995, and references therein).

Unlike the NEWSIPS and INES spectra, the fluxes resulting from the GEX spectra of PKS 0537–441 are consistent with the power-law which fits the quasi-simultaneous (within few days) optical data (see also below). Therefore, we have decided to adopt the GEX extraction for the 1995 IUE spectra. These have been calibrated according to Bohlin et al. (1990, SWP) and Cassatella et al. (1992, LWP), and have been binned in 70–100  $\text{\AA}$ -wide wavelength intervals, after removing cosmic rays and by avoiding regions affected by spurious sunlight

( $\lambda \gtrsim 2800 \text{ \AA}$ ) and by large noise ( $1900 \text{ \AA} \lesssim \lambda \lesssim 2300 \text{ \AA}$ ). The binned spectra are reported in Fig. 3.

No emission lines superimposed on the UV continuum are detected in any of the IUE spectra. In particular, the Ly $\alpha$  and C IV lines, well detected by HST (see below), fall at the edges of the LWP range, where the sensitivity is poor. Moreover, the high state detected by IUE in 1995 (a factor of  $\sim 4$  higher than observed by HST), may have implied smaller line equivalent widths. A suggestion of C IV emission may be present in the average of the LWP spectra of PKS 0537–441 taken before 1988 (Courvoisier & Paltani 1992).

A power-law with slope  $\alpha_\nu \sim 1.2$  ( $f_\nu \propto \nu^{-\alpha_\nu}$ ) fits marginally well (reduced  $\chi^2 \simeq 2$ ) the 1995 optical and UV data at wavelengths longer than  $\sim 1700 \text{ \AA}$ , corrected for Galactic dust extinction ( $E_{B-V} = 0.037 \text{ mag}$ , Schlegel et al. 1998) with the law by Cardelli et al. (1989). The spectral index is in agreement with that determined for the optical spectra only (Scarpa & Falomo 1997). The LWP spectrum appears steeper than this, which may account for the not completely satisfactory value of the  $\chi^2$ . The discrepancy may be due to the limited quality of the IUE LWP data, and to the non-strict simultaneity.

The UV points at wavelengths shorter than  $1700 \text{ \AA}$  clearly deviate from the optical-to-UV power-law behavior and

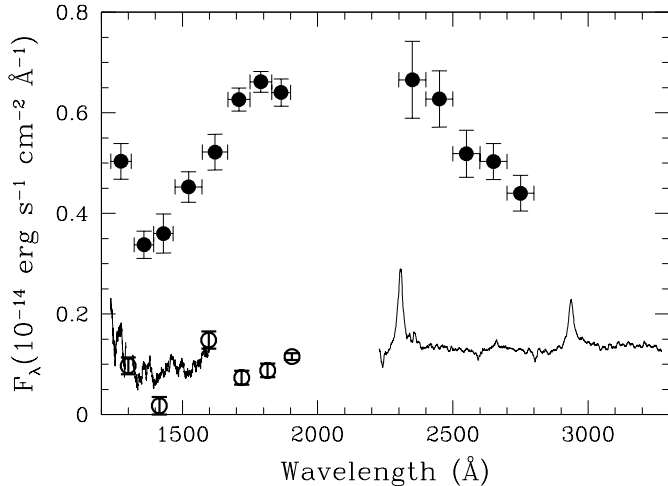


**Fig. 3.** IUE (circles) and HST FOS (solid curves) spectra of PKS 0537–441 not corrected for Galactic extinction. The IUE data refer to a bright (January 1995, filled circles) and a faint (April 1982, open circles) state. The FOS G130H and G270H spectra, smoothed over wavelength intervals of 12.5 and 5 Å, respectively, sample a low state (July and September 1993, respectively), comparable to that observed by IUE in 1982. Note that the strongest emission lines, Ly $\alpha$  and C IV, well visible in the HST spectrum, occur out of the usable wavelength region of the IUE data.

suggest a flux deficit by up to 50% at  $\sim 1350$  Å (Fig. 3). This feature is seen independent of the method adopted for spectral extraction. However, we note that the background has an irregular shape along the dispersion direction, and possible instrumental effects cannot be excluded. The only other SWP spectrum available for PKS 0537–441 (25 April 1982, Fig. 3) obtained at a very faint state, has insufficient signal-to-noise ratio to confirm or disprove the reality of the feature (see also Lanzetta et al. 1995). Moreover, a similar dip is not seen in the HST FOS G130H spectrum (see below), which has a level comparable to that of the 1982 IUE spectrum (Fig. 3), but a much better signal-to-noise ratio. Therefore, we do not consider this feature in the analysis of the multiwavelength energy distribution (Sect. 3).

PKS 0537–441 was observed by the HST Faint Object Spectrograph (FOS) in July and September 1993 (pre-COSTAR) with the G130H and G270H gratings, respectively (Table 1). We retrieved both spectra from the HST archive<sup>3</sup> (see also Bechtold et al. 2002). The G130H spectrum, which is rather noisy, presents a strong, sharp emission feature at  $\sim 1300$  Å that cannot be identified with any known emission (if at rest frame  $\lambda \sim 690$  Å). Because of this and the unusual shape we believe it is an instrumental effect. On the other hand, the G270H spectrum has a good signal-to-noise ratio, and exhibits broad, intense emission lines and Galactic interstellar absorptions (see Fig. 4).

We derived the central wavelength of each emission line by fitting the core of the features with Gaussians. Since the Ly $\alpha$  profile is slightly asymmetric due to a possible narrow absorption on the blue side and close to the center of the line,

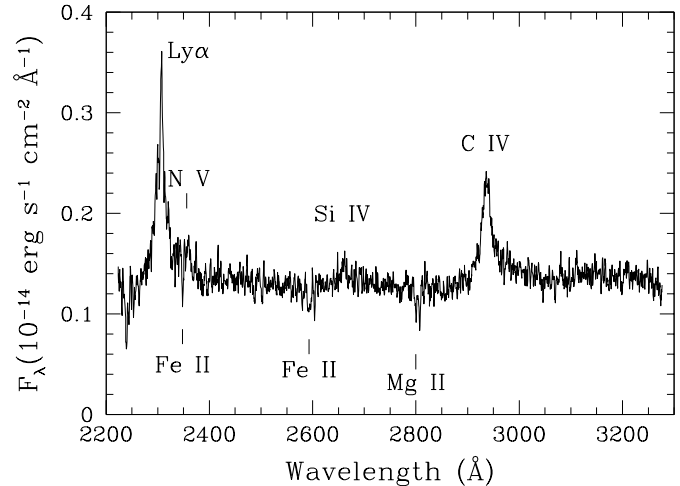


**Fig. 4.** FOS spectrum (G270H) of the blazar PKS 0537–441. Strong nuclear emission lines ( $z = 0.896$ ) and faint Galactic absorption features are clearly detected.

we derived the centroid of this line by excluding the inner portion of the core. On the basis of their measured central wavelengths (see Table 2), the emission lines are consistently identified with Ly $\alpha$ , Si IV, and C IV at  $z = 0.896 \pm 0.001$ . This is slightly larger than, but still consistent with historical redshift determination ( $z = 0.894$ , Peterson et al. 1976), based on Mg II $\lambda 2798$  emission, but only marginally consistent with  $z = 0.892 \pm 0.001$  given by Lewis & Ibata (2000), based on the Balmer line series and O III. The intensities and equivalent widths of the UV emission lines are reported in Table 2. After excluding the spectral regions affected by the lines, the UV continuum is well fitted by a power-law of index  $\alpha \approx 1.9$ .

We computed the continuum fluxes from the HST and IUE spectra by averaging the signal in 200-Å-wide bands in spectral regions free from lines, spurious features and noise, and corrected for Galactic extinction (see Table 1 and Fig. 2). The UV state of 1995 was about a factor 2 higher than in 1992 and a factor 4 higher than in 1993. The optical-to-UV spectrum in 1995 was flatter than the HST UV spectrum in 1993, consistent with the expected correlation of spectral flattening with brightening in synchrotron sources.

## 2.4. Optical

### 2.4.1. Spectroscopy

Optical CCD spectrophotometry was obtained in February 1991 (Falomo et al. 1994) and on 3, 5 and 7 February 1995 at the 1.5 m telescope of the European Southern Observatory (see Scarpa & Falomo 1997 for details of data acquisition, reduction and analysis, and Table 1 and Fig. 2 for the results). A 70% increase is apparent between 1991 and 1995 in the optical flux. We detected a monotonic increase of about 70% during the 3 nights of the 1995 monitoring, accompanied by spectral hardening. The Mg II $\lambda 2798$  emission line is observed in all spectra, with non-significantly variable intensity,  $I_{\lambda} \approx 6 \times 10^{-15}$  erg s $^{-1}$  cm $^{-2}$  (not corrected for Galactic reddening,

<sup>3</sup> <http://archive.eso.org/wdb/wdb/hst/science/form>

**Table 2.** UV emission lines of PKS 0537–441.

Ion	$\lambda^a$	$EW^b$	$I^c$
Ly $\alpha$ $\lambda$ 1216	$2305.9 \pm 0.5$	$30 \pm 5$	$5.5 \pm 0.8$
Si IV $\lambda$ 1403	$2660.0 \pm 0.5$	$1.5 \pm 0.2$	$0.25 \pm 0.04$
C IV $\lambda$ 1549	$2937.0 \pm 0.5$	$22 \pm 3$	$3.6 \pm 0.5$

<sup>a</sup> Observed line wavelength in Å.

<sup>b</sup> Observed equivalent width in Å.

<sup>c</sup> Line intensity in  $10^{-14}$  erg s $^{-1}$  cm $^{-2}$ , corrected for Galactic extinction.

Scarpa & Falomo 1997; Treves et al. 1993. Note that the line intensity in the latter reference is misreported by a factor of 10).

### 2.4.2. Imaging

Stickel et al. (1988) reported the detection of extended optical emission surrounding PKS 0537–441, the characteristics of which led them to interpret it as a foreground disk galaxy along the line of sight to the blazar. However, this finding was not confirmed either by higher resolution optical images (Falomo et al. 1992; Heidt et al. 2002) and near-IR imaging (Kotilainen et al. 1998), consistent with the high redshift of the source and the relatively bright nucleus. This source was also imaged by HST using WFPC2 and F702W filter (Urry et al. 2000; Scarpa et al. 2000) and found to be unresolved. However, based on the analysis of the same HST images, Lewis & Ibata (2000) claim the finding of faint non-axisymmetric extended emission. This result was obtained from the subtraction of a scaled PSF constructed with the Tiny Tim software (Krist 1995). While Tiny Tim offers a reliable description of the central part of the HST-WFPC2 PSF it does not account for the emission due to the large angle scattered light (particularly for the Planetary Camera) that produces extra emission at radii larger than  $\sim 2$  arcsec, as illustrated in Fig. 5 (see also Scarpa et al. 2000). We therefore believe that the extra light reported by Lewis & Ibata (2000) is fully accounted for by the contribution of the scattered light. Moreover, we note that no signature of stellar features has been reported in the optical spectra of PKS 0537–441 to support the presence of a foreground galaxy (Stickel et al. 1988; Lewis & Ibata 2000). Therefore, the microlensing hypothesis does not appear tenable (see also Romero et al. 2000).

### 2.5. Millimeter

PKS 0537–441 was monitored during the year 1995 with the 15-metre Swedish-ESO Submillimetre Telescope (SEST) at La Silla, Chile (Tornikoski et al. 2002, in preparation). Observations were made at 90 GHz using a dual polarization Schottky receiver, and at 230 GHz using a single channel bolometer. More details on the observations and data reduction can be found in Tornikoski et al. (1996). The sampling is only marginally simultaneous with EGRET. The fluxes obtained closest in time with the EGRET observation are reported in Table 1, along with errors, which consist of the

standard deviation among the individual daily measurements and the estimated effect of the calibration and pointing uncertainties.

These data suggest a very moderate brightening in the radio flux curve at 90 GHz just about the time of the multiwavelength campaign, but not comparable to the 1994 outburst (Tornikoski et al. 1996). In the 230 GHz data no changes can be seen from December 1994 to the end of February 1995, but the sampling is too sparse to completely exclude the possibility of a minor burst similar to that seen in the 90 GHz curve (see Tornikoski et al. 1996).

## 3. Discussion

In Fig. 2 we have reported the broad-band spectral energy distributions of PKS 0537–441 constructed with quasi-simultaneous data from the millimetric to the  $\gamma$ -ray frequencies (see Table 1). In addition, we have reported the unpublished BeppoSAX spectrum. The multiwavelength state of PKS 0537–441 in January–February 1995 was one of the brightest recorded for this source during the lifetime of EGRET (cf. Tornikoski et al. 1996; Falomo et al. 1994; Hartman et al. 1999). The comparison of  $\gamma$ -ray detection and optical flux of 1991 and the EGRET upper limit and UV flux of 1992 is suggestive of little or no multiwavelength variability between the two epochs. The increase of the optical-to-UV flux from the 1991–1992 to the 1995 level corresponds to a variation of similar amplitude (a factor of  $\sim 2$ ) in the  $\gamma$ -rays, or only slightly larger. The flat BeppoSAX spectrum suggests that a single emission component dominates in the energy band 0.1–30 keV.

PKS 0537–441 exhibits the typical double-humped multi-wavelength spectral shape of “Low-frequency-peaked” blazars (Padovani & Giommi 1995; Sambruna et al. 1996; Fossati et al. 1998): the first component peaks at wavelengths longer than the optical (likely in the far-infrared, as suggested by the IRAS data, taken at a much earlier epoch, Impey & Neugebauer 1988) and is due to synchrotron radiation. The second component, which peaks around  $\sim 10^{22}$ – $10^{24}$  Hz (Fig. 2) and is a factor  $\sim 6$  more powerful than the synchrotron maximum, is probably produced via inverse Compton scattering between relativistic electrons and synchrotron photons (Maraschi et al. 1992; Maraschi et al. 1994b; Bloom & Marscher 1993) or external photons (broad emission line region or accretion disk, Dermer & Schlickeiser 1993; Sikora et al. 1994).

The overall energy distribution of PKS 0537–441, the inverse-Compton dominance, and the presence of optical and UV emission lines suggest that external Compton upscattering may be significant with respect to the synchrotron self-Compton process in producing the high energy emission (Ghisellini et al. 1998; Ghisellini 2001). To model the broad-band energy distribution of PKS 0537–441 we have assumed that the emission is produced in a region filled by relativistic particles which radiate at low energies via synchrotron, and upscatter both synchrotron photons and accretion disk photons reprocessed in the broad emission line region. We have not included the direct contribution of the accretion disk to the population of seed photons to be upscattered by the jet electrons,

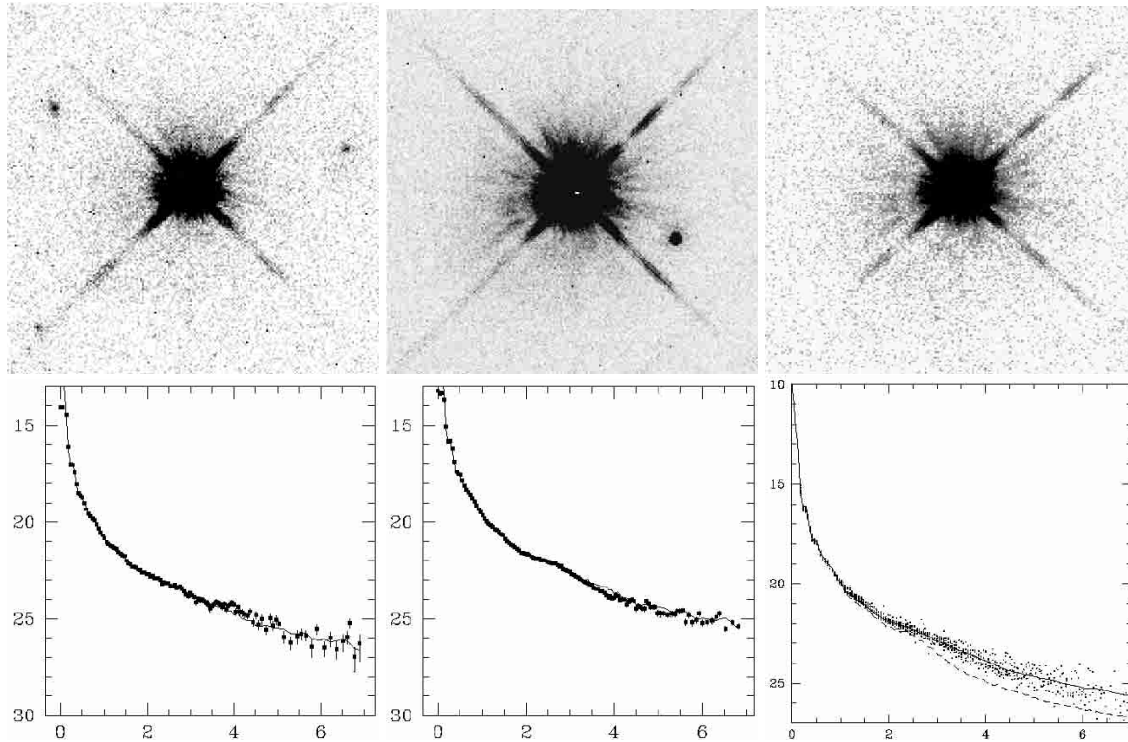


**Fig. 5.** The upper panels show, from left to right, the HST Planetary Camera images in F702W filter of PKS 0537–441, the unresolved blazar H 1722+119, and a star (the angular size of each field is  $9''.2 \times 9''.2$ ). The lower panels report, from left to right, the PSF model fit (solid curve), including the contribution of scattered light, to the observed profiles of surface brightness (in  $\text{mag arcsec}^{-2}$ ) vs. radius (in arcsec) for PKS 0537–441, H 1722+119, and many stars (dots). In the third lower panel we also report, for comparison, the Tiny Tim PSF model (dashed curve), which is clearly unable to describe the profile of point-like sources at radii larger than  $\sim 2$  arcsec (see also Scarpa et al. 2000).

because those would be highly redshifted in the frame of the blob, which is emitting at a distance of  $\sim 0.3$  pc (see caption to Fig. 2) from the jet base (Sikora et al. 1994). The size of the emitting region has been constrained with the variability time scale in  $\gamma$ -rays ( $\sim 2$  days); the electron energy distribution is modeled with a double power-law (see Tavecchio et al. 2000 and Ballo et al. 2002 for more details of the model). The low state model has been constrained with the BeppoSAX spectrum and with the 1991–1992 optical and  $\gamma$ -ray data, while the high state model reproduces the 1995 multiwavelength data. Note that the ROSAT spectral measurement of April 1991, which is affected by a large uncertainty, is consistent both with the low and high state model curves. The IRAS data are marginally consistent with the high state model.

The difference between the two model curves (reported in Fig. 2; see caption for the model parameters) is solely determined by a change in the Lorentz factor of the relativistic plasma bulk motion (increasing by 10% from the low to the high state) and in the index of the upper branch of the electron energy distribution ( $n_2$  in the notation of Ballo et al. 2002, slightly flatter in the brighter state, see caption to Fig. 2). Under our assumption that the high energy component results from the contribution of both synchrotron-self Compton and external Compton mechanisms, the variation of the bulk Lorentz factor would produce a correlation between the variability amplitude of the synchrotron and inverse Compton components which is intermediate between linear and half-cubic (Ghisellini & Maraschi 1996). This is consistent with the observations,

although the difficulty of exactly locating the peaks of the emission components, the non-strict simultaneity of the optical-to-UV spectra and the rapid  $\gamma$ -ray flare seen at the end of the EGRET viewing period make the fit results only indicative.

From our measured UV line intensities reported in Table 2 and from dereddened MgII emission line intensity (Sect. 2.4.1), assuming  $H_0 = 65 \text{ km s}^{-1} \text{ Mpc}^{-1}$ ,  $\Omega_m = 0.3$ ,  $\Omega_\Lambda = 0.7$ , we derive a total line luminosity  $L_{\text{BLR}} \sim 4.7 \times 10^{44} \text{ erg s}^{-1}$  (the other observed optical emission lines are sufficiently weak that their contribution to the line luminosity is not significant, see Lewis & Ibatova 2000). Using this and the external photon density assumed in our model,  $U_{\text{ext}} = 6 \times 10^{-3} \text{ erg cm}^{-3}$ , we can evaluate the size of the broad line region,  $R_{\text{BLR}} \approx 7.9 \times 10^{17} \text{ cm}$ . As an independent check, we have considered the empirical relationship determined by Kaspi et al. (2000) between the size of the broad line region and the luminosity of the thermal continuum at  $5100 \text{ \AA}$  in quasars. Assuming a covering factor of the broad line clouds of 10%, we can estimate the disk luminosity to be  $L_{\text{disk}} \sim 4.7 \times 10^{45} \text{ erg s}^{-1}$ . This value is consistent with the approximate upper limit which can be derived from the broad band spectrum,  $\sim 2 \times 10^{46} \text{ erg s}^{-1}$ . After accounting for a factor of  $\sim 3$  difference between a bolometric and a monochromatic disk output, we find that our disk luminosity estimate implies, according to Kaspi et al.'s formula,  $R_{\text{BLR}} \approx 5.8 \times 10^{17} \text{ cm}$ , well consistent, given the uncertainties, with the size we have determined based on the observed  $L_{\text{BLR}}$  and on the assumed photon density. We finally note that our observed  $L_{\text{BLR}}$  is about a factor 4 lower than that estimated for this source by

Celotti et al. (1997), based on an old measurement of the MgII emission only.

The validity and origin of the spectral dip seen in the IUE spectrum of January 1995 at wavelengths shorter than 1700 Å remain to be established. Assuming it to be real, it could be qualitatively described by an absorption edge or broad trough, and may be identified with neutral hydrogen ionization discontinuity (Lyman limit) at the redshift of the source or with Ly $\alpha$  forest blanketing up to a maximum redshift of  $\sim 0.4$ . Continuum decrements shortward of Ly $\alpha$  emission, Lyman limit systems and damped Ly $\alpha$  absorption features have been reported in few blazars at redshifts  $0.5 \lesssim z \lesssim 1.5$  (e.g., PKS 0637–752, Cristiani et al. 1993; PKS 0735+178, PKS 2223–052 Courvoisier & Paltani 1992; Lanzetta et al. 1995). Absorption features have recently been reported also in X-ray blazar spectra (Tavecchio et al. 2000). The host galaxy or the halos of the galaxies located in the vicinity of PKS 0537–441 and at similar redshift (projected distances of  $\sim 30$  kpc, Heidt et al. 2002) may be responsible for absorption in the bluer part of the UV nuclear spectrum. Using the photoelectric cross-section computed by Rumph et al. (1994) to model the interstellar opacity at extreme UV wavelengths, we estimated that in the case of Lyman continuum absorption the equivalent intrinsic  $N_{\text{HI}}$  would be about 3 orders of magnitude lower than the Galactic  $N_{\text{HI}}$  in the direction of the blazar, and therefore its effect on the X-ray spectrum would be undetectable. Alternatively, the FOS G130H spectrum may suggest resemblance with those of Broad Absorption Line quasars (e.g., Hamann & Ferland 1999; Arav et al. 2001), so that, in the lower resolution IUE SWP spectrum, many broad features would appear blended in a unique edge.

Higher signal-to-noise ratio data (ideally HST STIS spectra simultaneously covering the wavelength range 1100–2700 Å) would be necessary to confirm the presence of the feature and accurately model it. The nuclear emission and environmental characteristics of the blazar PKS 0537–441 make it a case study for future  $\gamma$ -ray missions like AGILE and GLAST and for the NGST, respectively.

*Acknowledgements.* We thank W. Wamsteker and the IUE Observatory staff for their support of this project, C. Morossi for useful comments on the IUE spectral response, C. Imhoff, K. Levay and P. Padovani for assistance with IUE and HST archives, and P. Goudfrooij, M. Massarotti, P. Molaro, and M. Stiavelli for helpful suggestions. This work is partly supported by COFIN 2001/028773, ASI-IR-35. This research has made use of the NASA/IPAC Extragalactic Database (NED) which is operated by the Jet Propulsion Laboratory, California Institute of Technology, under contract with the National Aeronautics and Space Administration.

## References

- Arav, N., de Kool, M., Korista, K., et al. 2001, *ApJ*, 561, 118
- Ballo, L., Maraschi, L., Tavecchio, F., et al. 2002, *ApJ*, 567, 50
- Bechtold, J., Dobrzycki, A., Wilden, B., et al. 2002, *ApJS*, 140, 143
- Bersanelli, M., Bouchet, P., Falomo, R., & Tanzi, E. G. 1992, *AJ*, 104, 28
- Bloom, S. D., & Marscher, A. P. 1993, in *Compton Gamma-Ray Observatory*, ed. M. Friedlander, N. Gehrels, & D. J. Macomb (New York: AIP), AIP Proc., 280, 578
- Bloom, S. D., Bertsch, D. L., Hartman, R. C., et al. 1997, *ApJ*, 490, L145
- Boella, G., Butler, R. C., Perola, G. C., et al. 1997, *A&AS*, 122, 299
- Bohlin, R., Harris, A. W., Holm, A. V., & Gry, C. 1990, *ApJS*, 73, 413
- Caplinger, J. 1995, *NASA IUE Newsletter*, 55, 17
- Cardelli, J. A., Clayton, G. C., & Mathis, J. S. 1989, *ApJ*, 345, 245
- Cassatella, A., Lloyd, C., & Gonzalez-Riestra, R. 1988, *ESA IUE Newsletter*, 31, 13
- Celotti, A., Padovani, P., & Ghisellini, G. 1997, *MNRAS*, 286, 415
- Courvoisier, T. J.-L., & Paltani, S. 1992, *IUE-ULDA Access Guide No. 4, Active Galactic Nuclei*, ESA SP 1153, vols. A and B
- Cristiani, S., Giallongo, E., Buson, L. M., Gouiffes, C., & La Franca, F. 1993, *A&A*, 268, 86
- Cruz-Gonzalez, I., & Huchra, J. P. 1984, *AJ*, 89, 441
- Dermer, C., & Schlickeiser, R. 1993, *ApJ*, 416, 458
- Edelson, R. A., Pike, G. F., Saken, J. M., Kinney, A., & Shull, J. M. 1992, *ApJS*, 83, 1
- Falomo, R., Melnick, J., & Tanzi, E. G. 1992, *A&A*, 255, L17
- Falomo, R., Bersanelli, M., Bouchet, P., & Tanzi, E. G. 1993a, *AJ*, 106, 11
- Falomo, R., Treves, A., Chiappetti, L., et al. 1993b, *ApJ*, 402, 532
- Falomo, R., Scarpa, R., & Bersanelli, M. 1994, *ApJS*, 93, 125
- Fossati, G., Maraschi, L., Celotti, A., Comastri, A., & Ghisellini, G. 1998, *MNRAS*, 299, 433
- Frontera, F., Costa, E., dal Fiume, D., et al. 1997, *A&AS*, 122, 357
- Garhart, M. P., Smith, M. A., Levay, K. L., & Thompson, R. W. 1997, *IUE NASA Newsletter*, 57, 165
- Ghisellini, G., & Madau, P. 1996, *MNRAS*, 280, 67
- Ghisellini, G., & Maraschi, L. 1996, in *Blazar Continuum Variability*, ed. H. R. Miller, J. R. Webb, & J. C. Noble (ASP: San Francisco), ASP Conf. Ser., 110
- Ghisellini, G., Celotti, A., Fossati, G., Maraschi, L., & Comastri, A. 1998, *MNRAS*, 301, 451
- Ghisellini, G. 2001, in *X-ray Astronomy: Stellar Endpoints, AGN and the Diffuse X-ray Background*, Proc. of the Conference held in Bologna, 6–10 September 1999, ed. N. White, G. Malaguti, & G. G. C. Palumbo, AIP Conf. Proc., 599, 120 [astro-ph/0002355]
- Hamann, F., & Ferland, G. 1999, *ARA&A*, 37, 487
- Hartman, R. C. 1996, in *Blazar Continuum Variability*, ed. H. R. Miller, J. R. Webb, & J. C. Noble, ASP Conf. Ser., 110, 333
- Hartman, R. C., Webb, J. R., Marscher, A. P., et al. 1996, *ApJ*, 461, 698
- Hartman, R. C. 1999, in *BL Lac Phenomenon*, ed. L. O. Takalo, & A. Sillanpää, ASP Conf. Ser., 159, 199
- Hartman, R. C., Bertsch, D. L., Bloom, S. D., et al. 1999, *ApJS*, 123, 79
- Heidt, J., & Wagner, S. J. 1996, *A&A*, 305, 42
- Heidt, J., Fried, J., Hopp, U., et al. 2002, Proc. of the Workshop “QSO Hosts and Their Environments”, IAA, Granada, Spain, 10–12 January, 2001, ed. I. Marquez Perez et al. (Kluwer Academic Press), in press
- Impey, C. D., & Neugebauer, G. 1988, *AJ*, 95, 307
- Kaspi, S., Smith, P., Netzer, H., et al. 2000, *ApJ*, 533, 631
- Kotilainen, J. K., Falomo, R., & Scarpa, R. 1998, *A&A*, 336, 479
- Krist, J. 1995, in *Astronomical and Data Analysis, Software and Systems IV*, ed. R. A. Shaw, H. E. Payne, & J. J. E. Hayes (San Francisco: ASP), ASP Conf. Ser., 77, 349
- Lanzetta, K. M., Wolfe, A. M., & Turnshek, D. A. 1995, *ApJ*, 440, 435
- Lewis, G. F., & Iбата, R. A. 2000, *ApJ*, 528, 650
- Maraschi, L., Schwartz, D. A., Tanzi, E. G., & Treves, A. 1985, *ApJ*, 294, 615

- Maraschi, L., Ghisellini, G., & Celotti, A. 1992, *ApJ*, 397, L5
- Maraschi, L., Ghisellini, G., & Boccasile, A. 1994a, in *The Nature of Compact Objects in Active Galactic Nuclei*, Proc. of the 33rd Herstmonceux Conf., ed. A. Robinson, & R. Terlevich (Cambridge University Press), 381
- Maraschi, L., Grandi, P., Urry, C. M., et al. 1994b, *ApJ*, 435, L91
- Mattox, J. R., Wagner, S. J., Malkan, M., et al. 1997, *ApJ*, 476, 692
- McBreen, B. 1979, *A&A*, 71, L19
- Michelson, P. F., Lin, Y. C., Nolan, P. L., et al. 1992, *IAU Circ.* 5470
- Mukherjee, R., Bertsch, D. L., Bloom, S. D., et al. 1997, *ApJ*, 490, 116
- Murphy, E. M., Lockman, F. J., Laor, A., & Elvis, M. 1996, *ApJS*, 105, 369
- Nichols, J. S., & Linsky, J. L. 1996, *AJ*, 111, 517
- O'Brien, P. T., Gondhalekar, P. M., & Wilson, R. 1988, *MNRAS*, 233, 845
- Padovani, P., & Giommi, P. 1995, *ApJ*, 444, 567
- Peterson, B. A., Jauncey, D. L., Wright, A. E., & Condon, J. J. 1976, *ApJ*, 207, L5
- Romero, G. E., Combi, J. A., & Colomb, F. R. 1994, *A&A*, 288, 731
- Romero, G. E., Surpi, G., & Vucetich, H. 1995, *A&A*, 301, 641
- Romero, G. E., Cellone, S. A., & Combi, J. A. 2000, *AJ*, 120, 1192
- Romero, G. E., Cellone, S. A., Combi, J. A., & Andruchow, I. 2002, *A&A*, 390, 431
- Rumph, T., Bowyer, S., & Vennes, S. 1994, *AJ*, 107, 2108
- Sambruna, R. M., Maraschi, L., & Urry, C. M. 1996, *ApJ*, 463, 444
- Scarpa, R., & Falomo, R. 1997, *A&A*, 325, 109
- Scarpa, R., Urry, C. M., Falomo, R., Pesce, J. E., & Treves, A. 2000, *ApJ*, 532, 740
- Scarsi, L. 1993, *A&AS*, 97, 371
- Schlegel, D. J., Finkbeiner, D. P., & Davis, M. 1998, *ApJ*, 500, 525
- Sefako, R. R., de Jager, O. C., & Winkler, H. 2000, *Proceedings of the Heidelberg International Symposium on High Energy Gamma-Ray Astronomy* [astro-ph/0010263]
- Sikora, M., Begelman, M., & Rees, M. J. 1994, *ApJ*, 421, 153
- Sreekumar, P., Bertsch, D. L., Dingus, B. L., et al. 1996, *ApJ*, 464, 628
- Sreekumar, P., Hartman, R. C., Mukherjee, R., & Pohl, M. 2001, in *Gamma-Ray Astrophysics 2001*, ed. S. Ritz, N. Gehrels, & C. R. Shrader (Melville NY: AIP), AIP Conf. Proc., 587, 314
- Stickel, M., Fried, J. W., & Kühr, H. 1988, *A&A*, 206, L30
- Tanzi, E. G., Barr, P., Bouchet, P., et al. 1986, *ApJ*, 311, L13
- Tavecchio, F., Maraschi, L., Ghisellini, G., et al. 2000, *ApJ*, 543, 535
- Thompson, D. J., Bertsch, D. L., Fichtel, C. E., et al. 1993, *ApJ*, 410, 87
- Thompson, D. J., Bertsch, D. L., Dingus, B. L., et al. 1996, *ApJS*, 107, 227
- Tingay, S. J., Edwards, P. G., Costa, M. E., et al. 1996, *ApJ*, 464, 170
- Tornikoski, M., Valtaoja, E., Teräsranta, H., et al. 1996, *A&AS*, 116, 157
- Tornikoski, M., Jussila, I., Johansson, P., Lainela, M., & Valtaoja, E., 2001, *AJ*, 121, 1306
- Treves, A., Belloni, T., Falomo, R., et al. 1993, *ApJ*, 406, 447
- Urry, C. M., Maraschi, L., Edelson, R., et al. 1993, *ApJ*, 411, 614
- Urry, C. M., & Reichert, G. A. 1988, *IUE Newsletter*, 34, 95
- Urry, C. M., Scarpa, R., O'Dowd, M., et al. 2000, *ApJ*, 532, 816
- von Montigny, C., Bertsch, D. L., Chiang, J., et al. 1995, *ApJ*, 440, 525
- Wehrle, A. E., Pian, E., Urry, C. M., et al. 1998, *ApJ*, 497, 178